Fall September 1, 2019

An Artificial Neural Network Model For Predicting The Greenhouse Heat Requirement in Adana Climate Conditions

Ali Çaylı, *University of Kahramanmaras Sutcu Imam*

© by PSP Volume 28 – No. 9/2019 pages 6537-6548 Fresenius Environmental Bulletin

AN ARTIFICIAL NEURAL NETWORK MODEL FOR PREDICTING THE GREENHOUSE HEAT REQUIREMENT IN ADANA CLIMATE CONDITIONS

Ali Cayli*

Kahramanmaras Sutcu Imam University, Vocational School of Turkoglu, Kahramanmaras, Turkey

ABSTRACT

In addition to the application of modern cultivation techniques and technological solutions, plant quality and yield can be increased through heating in a greenhouse during the cold winter months. Within a greenhouse heating system, the greenhouse heat requirement is the most important parameter for efficient operation. Calculations of the heat requirement should take into consideration the long-term average temperature and the regional climatic conditions. Based on these calculations, the greenhouse heating system power and production costs can be predicted.

In this study, an artificial neural network (ANN) model which can be used for planning, feasibility studies, and automation systems was developed to estimate the heat requirement of modern greenhouses. In this model, the performance of the activation and training algorithms was determined with the aim to provide heat requirement estimates that are close to actual consumption values.

The fuel consumption data from a commercial greenhouse operation in Adana for the 2015 production year and climatic data from an official meteorological station were used to test the model. By comparing different activation functions and training algorithms, the most suitable algorithm for the model was able to be determined. A total of eight models were then created and their performances compared statistically. As a result, a model that was able to produce estimates that were very close to the actual fuel consumption was developed.

KEYWORDS:
Artificial neural networks, Greenhouse heating, Greenhouse heat requirement, Greenhouses

INTRODUCTION

Artificial intelligence (AI) can be defined as the mathematical imitation of the learning and decision-making characteristics of the human brain. Various models have been employed in artificial intelligence applications; one of these is artificial neural networks (ANNs), an AI system that provides a mathematical analysis of everyday problems using algorithms based on the human brain. An ANN is a black box model that consisting of input-output parameters and the relationships between them. This model does not consider the input, output, causes. Cognitive scientists and neuroscientists aim to understand the functioning of the brain; to achieve this, they build models of neural networks and conduct simulation studies. However, artificial intelligence is a component of computer science and the primary objective here is to build useful systems, as in any domain of engineering [1].

In its most general form, a neural network is a machine that is designed to model the way in which the brain performs a particular task or function of interest; the network is usually implemented by using electronic components or is simulated in software on a digital computer [2]. Machine learning is the act of programming computers in a way that optimizes a performance criterion using example data or past experience [1]. The main attraction of troubleshooting using ANNs is the ability to generalize learning and learned information. The ability to engage in network capacity learning with a small set of samples and the provision of consistent answers for unknown data is proof that ANN's abilities have gone beyond mapping only the input and output relationships. ANNs can remove information that is not expressly granted by the samples.

In previous applications, ANNs have been employed to generate hourly temperature estimates [3], recognize species of butterflies and insects [4, 5], determine precipitation and spatial distributions [6], predict natural disasters using climate data [7], predict soil temperatures in different regions and at different depths [8], estimate water levels in lakes using hydrological data [9], classify farmland [10], estimate the yield of crops [11], completion of missing data in soil property measurement data [12], spatially model soil salinity using wetness indices [13], control weeds in sugar beet crops using an intelligent spraying robot based on image processing [14], determine the level of underground water [15, 16], predict the number of flowers in fruit trees [17], predict fungal infections in pumpkin plants [18], predict nitrate pollution in groundwater [19], classify the maturity of tomatoes [20], estimate the impact of herbal

production on annual gross national turnover using climate data [21], classify cultivated land based on unmanned aerial images [22], evaluate water and energy cycles through the monitoring of long-term meteorological variables such as precipitation, air temperature, proportional and absolute humidity, air pressure, wind velocity, and shortwave radiation [23], determine sowing patterns using images obtained by remote sensing [24, 25], predict solar radiation [26], estimate evapotranspiration [27], evaluate drought reduction options [28], predict and warn of frost in greenhouses [29], estimate tractor fuel consumption [30], estimate the amount of energy consumed in agricultural production and the production of greenhouse gas emissions [31], and identify soil erosion classes and determine sensitivity to erosion [32, 33].

In the agricultural sector, greenhouses are the farming activity that has the highest energy requirements per unit area. Greenhouses are also desirable to be structurally durable [34]. If there is not enough insulation in a heated greenhouse, more heat energy will be needed during cold periods. For example, the regular heating costs of heat-protected greenhouses on the Mediterranean coastline account for 20% of overall production costs [35].

The greenhouse heat requirement is calculated according to European Union standards depending on the size and type of greenhouse, the equipment used, and the temperature required for the plants. However, there are different methods to determine the heat energy requirement in greenhouses [35]. Canakci, et al. [36] calculated the heat energy requirement for Antalya by taking into consideration the temperature averages at night and the night length, while Damrath and Klein [37] calculated the heat energy requirement for Trier (Germany) using hourly values. Damrath [38] also determined the average of the temperature values over many years to calculate the annual heat energy requirement.

The average temperature is also used to calculate the heat energy requirement in greenhouses. However, during transition periods where average temperature is high and the temperature is kept low in the greenhouse, calculations using average temperature provide incorrect results [39]. For example, if the average outside temperature is 16 °C and the target greenhouse temperature is set at 16 °C, it could be concluded that the greenhouse does not need heating. However, the greenhouse temperature may be below or above the average of 16 °C. Therefore, it can be calculated that heat energy is not needed even though heating is needed at certain times of the day when the temperature is high [35].

Von Zabeltitz [40] reported the heat energy requirement for plastic greenhouses in the Mediterranean countries, using the method reported by Hallaire [41], determining the lowest temperature values and the day length values depending on the latitude of the region and finding that the heat energy requirement of a greenhouse can be calculated most accurately from hourly climatic measures.

Depending on the characteristics of the greenhouse, some solar energy is stored in the greenhouse. Heat energy stored throughout the day causes the temperature to rise in the greenhouse. Therefore, taking into consideration the heat storage properties of a greenhouse in the calculations for the daytime and nighttime, the rise of temperature in the series to be taken into consideration also provides more accurate results [42, 43].

In addition to many different parameters need to be taken into consideration when calculating the greenhouse heat requirement such as energy lost from the greenhouse, heat gain of the greenhouse, energy exchange resulting from the cultural activities. In order to simplify this process, an ANN model can be developed.

In this study, the temperature, relative humidity, and fuel consumption were measured for a commercial greenhouse operation in the province of Adana for the 2015 production year. Meteorological data for the region was used as input for an ANN model. The main objective was to determine the optimal ANN transfer function and to develop a model for the greenhouse heat requirement for Adana climate conditions.

MATERIALS AND METHODS

The research was conducted in a 20.160 m^2 plastic-covered modern commercial greenhouse in Adana. The roof of the greenhouse was single-layer PE plastic (200 μm) and the side walls were covered with double-layer polycarbonate (PC 10 mm). The dimensions of the greenhouse are given in Table 1.

TABLE 1
Dimensions of the greenhouse used in the study

Dimensions	Value	Unit
Span number	21	pieces
Span width	9.60	m
Length	100.00	m
Side wall height	5.00	m
Roof height	2.50	m
Ridge height	7.50	m
Side wall area	1000.00	m^2
Roof area	23617.76	m^2
Cover area	27340.32	m^2
Ground area	20160.00	m^2
A_H/A_G	1.36	-

The plastic greenhouse where the research was carried out is regularly heated by a coal boiler. The greenhouse heating pipes are 51 mm in diameter and located in plant rows and close to the greenhouse base. The fuel consumed during the production period (lignite coal) was recorded daily in kg and, for the energy conversion, the lower heat value of the

coal was 8.14 kWh kg^{-1}. The greenhouse temperature was controlled by regulating the water temperature using three-way distributor valves. In the greenhouse, tomatoes were grown in a soil-free culture at a density of 2.5 seedlings per square meter. Irrigation was conducted automatically using spaghetti drippers for each seedling. XLS 15 thermal screens (Ludwig Svensonn) were used for the conservation of heat energy within the greenhouse. The thermal screens were closed when solar radiation was 0 W/m^2 and gradually opened over the course of 30 minutes following sunrise. Outside climatic variables and the temperature, humidity, and solar radiation in the greenhouse were recorded as hourly averages. The greenhouse temperature was held at 16 °C using the control elements based on the measured climatic values. An official meteorological station (Adana 35 E 18; 37 N 01) was used for hourly temperature, solar radiation, and wind velocity measurements.

Traditionally, the greenhouse heat requirement is calculated according to the energy balance of the greenhouse. In other words, the energy gains and losses of the greenhouse are calculated then the amount of heat energy required for the desired internal temperature to be reached is determined. Accordingly, the greenhouse heat energy requirement can be calculated according to Equation 1, given by [35]:

$$Q = \sum_{n=1}^{8760}\left(\left(\left(\vartheta_{i_n} - \vartheta_{i,oH_n} - \Delta\vartheta_{Sp_n}\right) * k'_a * A_H * (1 - EE_{ES})\right) * t_{Si}\right) \quad (1)$$

where Q is the heat energy (Wh), ϑ_i is the indoor temperature (°C), $\vartheta_{i,oH}$ is the actual temperature in the unheated greenhouse (°C), $\Delta\vartheta_{Sp}$ is the temperature rise due to the features of the greenhouse (°C), k'_a is the overall heat requirement coefficient of the cover material (W m^{-2} K^{-1}), A_H is the surface area of the greenhouse cover (m^2), EE_{ES} is the heat savings from the thermal screens, n is the hours of the year, and t_{Si} is the time period (1 h).

The temperature rise ($\vartheta_{i,th}$) in an unventilated and unheated greenhouse is calculated according to Equation 2 [39, 44]:

$$\vartheta_{i,th} = \frac{q_{GS} * D_G * \eta * \mathrm{A_G}}{k'_a * (1 - EE_{ES}) * A_H} + \vartheta_a \quad (2)$$

where $\vartheta_{i,th}$ is the theoretical temperature in non-ventilated and non-heated greenhouse (°C), q_{GS} is the solar radiation (W m^{-2}), D_G is the transmittance of the cover material (%), η is the solar energy conversion factor (standard=0.7), $\mathrm{A_G}$ is the greenhouse floor area (m^2) and ϑ_a is the outside temperature (°C).

While determining the input parameters for the ANN, it is necessary to analyze the effect of the input parameters on the output value of the proposed model [45]. For this purpose, the influences on the heat flux and the greenhouse heat balance [46] are summarized in Figure 1.

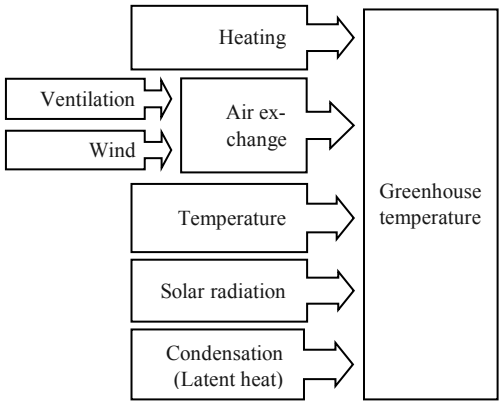

FIGURE 1
Parameters that affect the indoor temperature of a greenhouse

As shown in Figure 1, the greenhouse indoor temperature is influenced by air exchange, the outdoor air temperature, solar radiation, heating, ventilation, and wind. The ventilation rate is not used as an input parameter in the ANN model because ventilation cannot occur during active heating. Wind speeds were tested as an input parameter for the ANN model because heat losses from the surface of the greenhouse depend on the wind speed. In ANN applications, a multi-layer structure is widely used. The values are passed through an input layer, processed in a hidden layer, and forwarded to an output layer [45]. Without the hidden layer, a sensor can only perform linear tasks.

Figure 2 presents the general structure of the network tested in this paper. In most cases, ANN input and output parameters will have significantly different values. Log-sigmoid and tan-sigmoid activation functions are sensitive within the ranges [0,1] and [-1,1], respectively. Therefore, it is recommended that input and output data be scaled to avoid neuronal saturation. Scaling the data from the original range to the normalized range ([0,1] or [-1,1]) in accordance with the selected neuron transfer function is known as preprocessing. Both the input and output data must be normalized before network training [45].

The data used in the model was normalized according to Equation 3:

$$Xn = \frac{(x - x_{min}) \times r}{x_{max} - x_{min}} + r_{min} \quad (3)$$

where x is the value to be normalized, x_{min} and x_{max} are the minimum and maximum values of the data set, respectively, r is the normalization range, and r_{min} is the initial value of the normalization range.

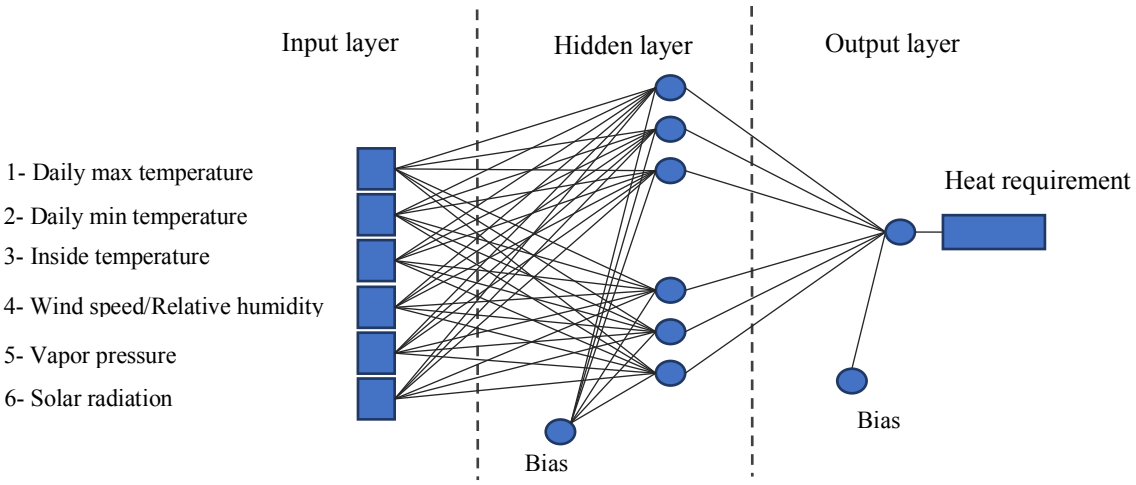

FIGURE 2
The structure of the proposed feed-forward ANN model

TABLE 2
The ANN model parameters

Parameters	Value
Input	6
Hidden layer	1
Number of neurons in the hidden layer	6
Output	1
Training algorithm	Levenberg-Marquardt *(trainlm)*
Training cycle	2000
Hidden layer activation function	Hyperbolic tangent sigmoid *(tansig)*
Output layer activation function	Linear *(purelin)*

A multilayer feed-forward neuron network was used in the model. The ANN model parameters are given in Table 2. The MATLAB software package [47] was used to train the ANN model. Demuth and Beale [47] have recommended the use of the sigmoid hidden layer activation function, which produces a linear output. Therefore, in this study, sigmoid activation functions were tested. During the production season, 144 days were heated. Of these, 85 were used to develop the model. In total, 70% of the input data was used to train the ANN model, and 30% was used for verification and testing.

In the ANN model, the estimated fuel consumption is calculated according to Equation 4:

$$Q = \sum_{i=1}^{k}\left(\frac{2}{1+e^{-2(N_i)}} - 1\right) \times l_i + \theta, \quad (4)$$

where k is the number of neurons in the hidden layer, l_i is the weight vector of the connections between the hidden and output layer, θ is the output layer bias (threshold), and N_i is the calculated neuron value.

In this study, sigmoid (logsig) and tangent hyperbolic sigmoid (tansig) activation functions in the hidden layer and a linear (purelin) activation function in the output layer were used. The general form of these activation functions are as follows:

$$f(x) = \frac{1}{1+e^{-x}} \quad (5)$$

$$f(x) = \left(\frac{2}{1+e^{-2x}}\right) - 1 \quad (6)$$

$$f(x) = x\,. \quad (7)$$

The tansig transfer function (Equation 6) used in ANN applications is associated with a bipolar sigmoid with an output between -1 and +1, and this is mathematically equivalent to tanh (x). Although there are very small numerical differences in the results, this function is faster. Therefore, it is a suitable option for neural networks where speed is more important than the exact form of the transfer function [48].

In an ANN model, the value of the neurons in the hidden layer is determined by adding the bias (threshold) to the weighted totals of the input vectors. This is expressed in Equation 8:

$$N = \sum_{i=1}^{n} x_i \times w_i + \theta_i, \quad (8)$$

where n is the input parameter number, w_i is the input vector of the connections between the input and hidden layer, x_i is the input vector, and, θ_i is the bias (threshold) of the first neuron in the hidden layer.

Ten different training algorithms for the log-sigmoid and tan-sigmoid activation functions were tested to determine the optimal activation function for the ANN model. In the tests, fuel consumption

was used as the output parameter with one hidden layer and six input parameters. The maximum number of iterations was 1000, the error value was 0.00001, and the epoch value was 100.

After determining the optimal activation function and training algorithm, eight different models were created. In these models, climatic parameters such as ambient temperature, wind velocity, proportional humidity, solar radiation, and steam pressure were used in different combinations as input vectors. The training cycle was repeated 2000 times for each model. At the end of the training cycle, the model with the smallest mean square error (MSE) was chosen as the best performing model. The best performance model was then determined by comparing the root mean square error (RMSE), mean absolute percentage error (MAPE), mean absolute error (MAE), and determination coefficient (R^2) for the eight models. Accordingly, the model with a higher R^2 (Equation 10) and lower RMSE (Equation 9) and MAE (Equation 12) was chosen as the optimal model.

$$\mathrm{RMSE} = \sqrt{\frac{\sum_{i=1}^{n}\left(X_{i,A} - X_{i,P}\right)^2}{n}} \quad (9)$$

$$R^2 = 1 - \frac{\sum_{i=1}^{n}\left(X_{i,A} - X_{i,P}\right)^2}{\sum_{i=1}^{n}\left(X_{i,A} - X_M\right)^2} \quad (10)$$

$$\mathrm{MAPE} = \frac{1}{n}\frac{\sum_{i=1}^{n}\left|\frac{(X_{i,A} - X_{i,P})}{X_{i,A}}\right|}{n} \quad (11)$$

$$\mathrm{MAE} = \frac{1}{n}\sum_{i=1}^{n}\left|X_{i,A} - X_{i,P}\right| \quad (12)$$

In the equations above, n represents the number of observations, $X_{i,P}$ is the predicted output value, $X_{i,A}$ is the actual fuel consumption value, and X_M is the mean of the actual fuel consumption. MATLAB 7.12.0 software was used for the analysis on a computer running the Microsoft Windows 10 operating system with a 2.53 GHz Intel i5 CPU and 6 GB of RAM.

RESULTS AND DISCUSSION

In this study, the daily fuel consumption and climatic values for the 2015 growing season were used. According to the fuel consumption data (Figure 3), heating took place on 144 days between November 8, 2014 and March 31, 2015.

The results of the tests performed to determine the optimal activation function for the ANN model are provided in Tables 3 and 4.

For the log-sigmoid transfer function (Table 3), the most suitable training algorithm was the Levenberg-Marquardt (trainlm), which had the lowest RMSE and highest R^2. This algorithm is a modified Gauss-Newton algorithm that has been successfully used to solve non-linear smallest squares problems, including neural network training. In each iteration, it significantly outperforms variations with higher computational and memory requirements, basic back-propagation, and variable learning rates (e.g., education accuracy, convergence characteristics, general training period [49].

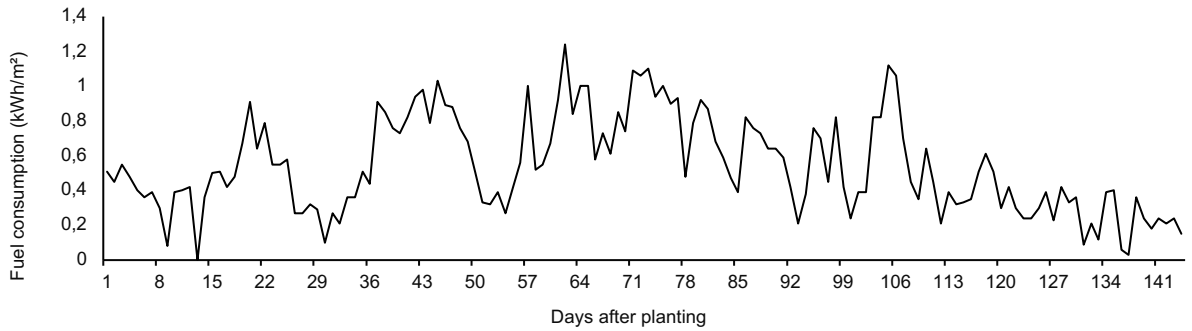

FIGURE 3
Fuel consumption for the greenhouse under investigation

TABLE 3
The performance of the training algorithms employing the log-sigmoid transfer function

Function	RMSE	R^2	Duration (s)	Number of iterations
Trainlm	0.20376	0.6752	1	229
Trainrp	0.21395	0.6065	1	290
Traingdm	0.24856	0.2396	26	25000
Traincgp	0.21858	0.5866	1	216
Trainscg	0.22713	0.4157	1	266
Trainbfg	0.21340	0.5484	1	344
Traincgb	0.21601	0.5841	1	258
Trainoss	0.21576	0.5836	1	365
Traincgf	0.23411	0.5101	1	290
Traingdx	0.21897	0.5384	1	773

TABLE 4
The performance of training algorithms employing the tan-sigmoid transfer function

Function	RMSE	R^2	Duration (s)	Number of iterations
Trainlm	0.11059	0.8350	1	208
Trainrp	0.11385	0.8239	1	333
Traingdm	0.13650	0.7491	27	25000
Traincgp	0.15038	0.6918	1	209
Trainscg	0.14466	0.7333	1	225
Trainbfg	0.14239	0.7235	1	232
Traincgb	0.13313	0.7698	1	242
Trainoss	0.11556	0.8213	1	326
Traincgf	0.14502	0.7156	1	222
Traingdx	0.16217	0.6443	1	334

TABLE 5
Performance of the model according to the number of hidden layers

Number of hidden layers		RMSE	R^2
Single layer	Training	0.06202	0.9411
	Validation	0.14293	0.8212
	Test	0.16358	0.6777
	All*	**0.09543**	**0.8658**
Two layers	Training	0.06695	0.9454
	Validation	0.15190	0.7869
	Test	0.13640	0.5718
	All	**0.09968**	**0.8651**
Three layers	Training	0.03837	0.9791
	Validation	0.16430	0.713
	Test	0.21500	0.6668
	All	**0.11050**	**0.8501**

In Table 4, the performances of 10 training algorithms using the tan-sigmoid transfer function are summarized. It can be observed that the optimal training algorithm is trainlm, which has the lowest RMSE and the highest R^2. When both transfer functions are evaluated together, the most suitable transfer function is tan-sigmoid, and the most suitable training algorithm is trainlm. The effect of increasing the number of hidden layers on the performance of the model was then tested using the tan-sigmoid transfer function and the trainlm training algorithm; the resulting RMSE and R^2 values are given in Table 5. It was found that increasing the number of hidden layers had no effect on the performance of the model. The best performance was observed in the single-layer model with six neurons.

The relationship between fuel consumption and the values used as input parameters is very important for the success of the model.

Figure 4 presents the regression graphs used to determine the relationship between the input and output parameters.

The R^2 for the relationships between fuel consumption and indoor temperature, daily minimum temperature, and atmospheric vapor pressure were 0.43, 0.35, and 0.30, respectively, while the R^2 for the relationship between fuel consumption and atmospheric relative humidity, solar radiation, and wind speed was 0.0005, 0.0266, and 0.0016, respectively. Descriptive statistics for the data set used for the ANN model are provided in Table 6, while the correlation analysis results for fuel consumption and other input parameters are summarized in Table 7.

According to these values, the climatic parameters that had the most significant effect on fuel consumption were daily minimum temperature, atmospheric vapor pressure, and daily maximum temperature value ($P<0.01$). The correlations between greenhouse fuel consumption and solar radiation and greenhouse indoor ambient temperature were also significant ($P<0.05$), while the correlations with outdoor ambient relative humidity and wind speed values were not significant ($P>0.05$).

The effect of some input parameters on fuel consumption may have been low due to the effective thermal insulation, the use of thermal screens, and the maximum wind speed in the region of 3 m/s. Indeed, Tantau [50] found that, for well-insulated greenhouses, wind has no effect on the heat requirement. In the proposed ANN model, using only the temperature parameters and vapor pressure as input parameters would be sufficient. However, to improve model performance, eight different models were created using all of the climatic parameters mentioned above and their performances compared. The results of these models are summarized in Table 8.

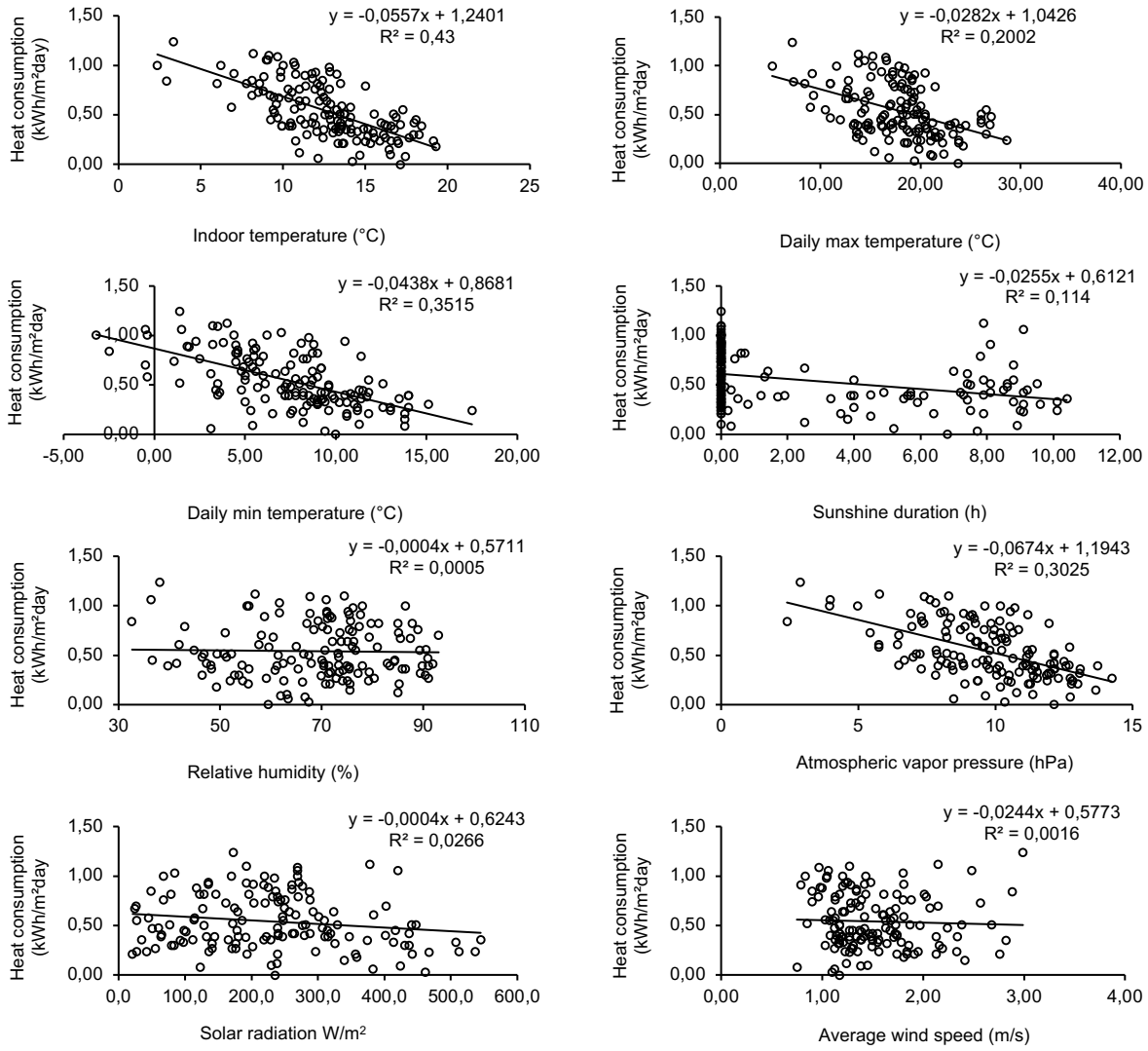

FIGURE 4
Relationships between key input and output parameters

TABLE 6
Descriptive statistics for the data set used in the study

Parameters	Minimum	Maximum	Average	Std. dev.
Daily maximum temperature (°C)	5.20	27.00	17.61	4.52
Daily minimum temperature (°C)	-3.20	15.10	7.30	4.05
Indoor temperature (°C)	13.85	22.45	17.21	1.21
Solar radiation (W/m²)	21.10	329.80	184.11	81.95
Relative humidity (%)	32.64	91.92	69.02	14.23
Vapor pressure (hPa)	2.40	14.20	9.73	2.44
Average wind speed (m/s)	0.80	3.00	1.41	0.46
Heat consumption (kWh/m²)	0.08	1.24	0.62	0.27

TABLE 7
Correlation analysis for the input and output parameters used in the ANN model

(** P<0.001)	Daily maximum temperature	Daily minimum temperature	Indoor temperature	Solar radiation	Relative humidity	Vapor pressure	Average wind speed
Pearson correlation coefficient	-0.439**	-0.698**	-0.245*	0.219*	-0.098	-0.640**	-0.005
Sig. (2-tailed)	0.000	0.000	0.024	0.044	0.373	0.000	0.962

TABLE 8
ANN model results (best of the 2000-run cycle)

Model	Independent variables	R^2	RMSE	MAPE
M1	Daily minimum temperature Indoor temperature	0.666	0.2677	25.5
M2	Daily minimum temperature Indoor temperature Vapor pressure	0.773	0.2207	21.3
M3	Daily maximum temperature Indoor temperature Vapor pressure	0.845	0.1827	15.9
M4	Daily minimum temperature Daily maximum temperature Indoor temperature Solar radiation	0.797	0.2094	24
M5	Daily minimum temperature Daily maximum temperature Indoor temperature Solar radiation Relative humidity	0.874	0.165	13.4
M6	Daily minimum temperature Daily maximum temperature Indoor temperature Solar radiation Vapor pressure	0.899	0.1485	13.4
M7 (*)	Daily minimum temperature Daily maximum temperature Indoor temperature Solar radiation Vapor pressure Relative humidity	0.945	0.1106	10.7
M8	Daily minimum temperature Daily maximum temperature Indoor temperature Solar radiation Vapor pressure Average wind speed	0.893	0.1534	18.2

TABLE 9
The results of the ANN model

	Train.	Valid.	Test	All
RMSE	0.103	0.129	0.122	0.111
MAPE (%)	9.118	13.719	14.609	10.662
MAE	0.045	0.056	0.058	0.049
R^2	0.947	0.929	0.947	0.945

As shown in Table 8, the M7 model, which was built using six inputs and the single output network structure presented in Figure 2, produced the best performance. Although the effects of relative humidity and solar radiation on fuel consumption are statistically very low (Table 7), the use of these parameters increased the performance of the model. The detailed results of the M7 model for the training, validation, and test data sets are given in Table 9, showing that its performance falls within acceptable limits.

The regression graphs of the estimated values found in the testing, training and verification stages of the model and the actual fuel consumption values are presented in Figure 5 and the actual and predicted greenhouse fuel consumption values are presented in Figure 6.

The weights for the input values used to calculate the neuron values between the input layer and the hidden layer are given in Table 10, while the weight values between the hidden layer and the output layer are given in Table 11.

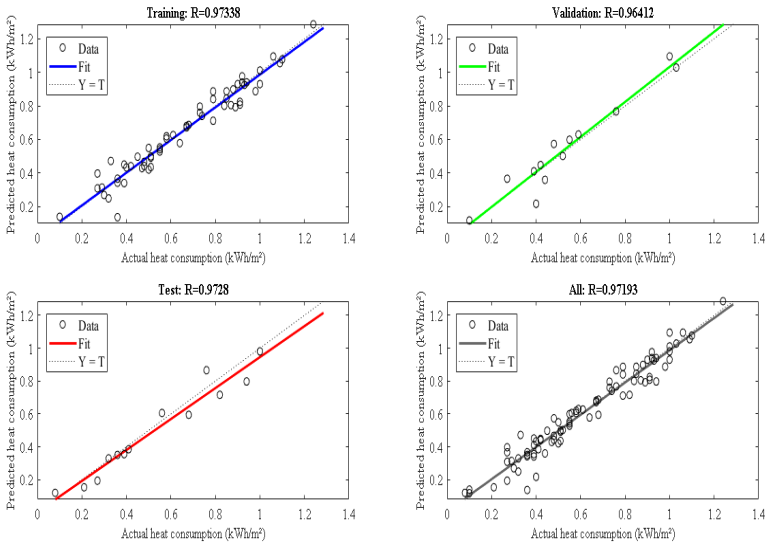

FIGURE 5
ANN model results

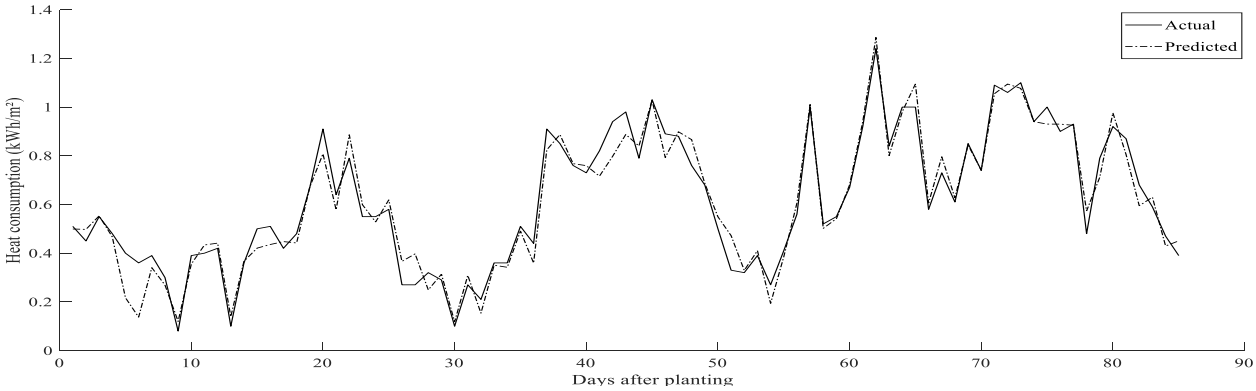

FIGURE 6
Actual and predicted greenhouse heat consumption

TABLE 10
Weight values between the input and hidden layers

	Weights						
Neurons in the input layer (i)	**W1i**	**W2i**	**W3i**	**W4i**	**W5i**	**W6i**	**Bias1**
1	-10.278	8.342	-28.792	-9.804	10.979	-7.673	-3.069
2	10.973	-1.985	24.011	-3.670	3.131	14.297	-4.714
3	19.052	-2.395	-14.309	-16.908	-20.005	11.510	-9.050
4	5.260	1.967	3.575	-0.488	9.229	-10.402	-2.256
5	0.840	-0.397	1.165	-0.045	-1.181	0.775	1.090
6	1.554	4.359	-16.987	-3.415	2.603	-8.274	-10.906

TABLE 11
Weight values between the hidden and output layers

Neurons in the input layer (i)	**Weights (Wi)**
1	0.3276
2	-0.2724
3	-0.2716
4	0.6206
5	1.1833
6	0.7517
Bias2	0.1856

The weight values in Tables 10 and 11 and the output activations obtained from Equation 8 are given in Equations 13-18. According to these results, the model for estimating fuel consumption is given in Equation 19. The input and output (i.e., fuel consumption estimation) values must be normalized using Equation 3.

$N_1 = -10{,}278X_1+8{,}342X_2-28{,}792X_3-9{,}804X_4+10{,}979X_5-7{,}673X_6-3{,}069$ (13)

$N_2 = 10{,}973X_1-1{,}985X_2+24{,}011X_3-3{,}67X_4+3{,}131X_5+14{,}297X_6-4{,}714$ (14)

$N_3 = 19{,}052X_1-2{,}395X_2-14{,}309X_3-16{,}908X_4-20{,}005X_5+11{,}51X_6-9{,}05$ (15)

$N_4 = 5{,}26X_1+1{,}967X_2+3{,}575X_3-0{,}488X_4+9{,}229X_5-10{,}402X_6-2{,}256$ (16)

$N_5 = 0{,}84X_1-0{,}397X_2+1{,}165X_3-0{,}045X_4-1{,}181X_5+0{,}775X_6+1{,}09$ (17)

$N_6 = 1{,}554X_1+4{,}359X_2-16{,}987X_3-3{,}415X_4+2{,}603X_5-8{,}274X_6-10{,}906$ (18)

Equation 19 is obtained by replacing the output activations in accordance with Equation 4. The greenhouse heat requirement estimate can then be calculated using Equation 19:

$$Q = \left(\left(\frac{2}{1+e^{-2(N1)}}-1\right)*0.3276+\left(\frac{2}{1+e^{-2(N2)}}-1\right)*-0.2724+\left(\frac{2}{1+e^{-2(N3)}}-1\right)*-0.2716+\left(\frac{2}{1+e^{-2(N4)}}-1\right)*0.6206+\left(\frac{2}{1+e^{-2(N5)}}-1\right)*1.1833+\left(\frac{2}{1+e^{-2(N6)}}-1\right)*0.7517+0.1856\right) \quad (19)$$

CONCLUSION

In this study, a prediction model for fuel consumption in a soilless tomato greenhouse was developed for the province of Adana using regional meteorological climatic data. An ANN model, variations of which have been successfully applied in many areas, can be used to estimate the greenhouse heat requirement. By adapting this method to specific greenhouse automation and control systems, it may be possible to both optimize fuel savings and plant climatic requirements. However, depending on the type of input data used, the proposed ANN model may not be valid in greenhouses with various spatial and structural arrangements. Therefore, heat requirement estimation models can be developed for greenhouses of different types or characteristics by following the methodology of this study.

REFERENCES

[1] Alpaydin, E. (2016) Machine learning: the new AI. Third edition ed. MIT Press, Massachusetts, 1-19.

[2] Haykin, S. (2009) Neural networks and learning machines. Pearson Upper Saddle River, NJ, USA, 2-3.

[3] Abdel-Aal, R.E. (2004) Hourly temperature forecasting using abductive networks. Engineering Applications of Artificial Intelligence. 17, 543-556.

[4] Zhu, L.Q., Ma, M.Y., Zhang, Z., Zhang, P.Y., Wu, W., Wang, D.D., Zhang, D.X., Wang, X. and Wang, H.Y. (2017) Hybrid deep learning for automated lepidopteran insect image classification. Oriental Insects. 51, 79-91.

[5] Espinoza, K., Valera, D.L., Torres, J.A., Lopez, A. and Molina-Aiz, F.D. (2016) Combination of image processing and artificial neural networks as a novel approach for the identification of Bemisia tabaci and Frankliniella occidentalis on sticky traps in greenhouse agriculture. Computers and Electronics in Agriculture. 127, 495-505.

[6] Zambrano, F., Wardlow, B., Tadesse, T., Lillo-Saavedra, M. and Lagos, O. (2017) Evaluating satellite-derived long-term historical precipitation datasets for drought monitoring in Chile. Atmospheric Research. 186, 26-42.

[7] Yu, X.B. (2017) Disaster prediction model based on support vector machine for regression and improved differential evolution. Natural Hazards. 85, 959-976.

[8] Yener, D., Ozgener, O. and Ozgener, L. (2017) Prediction of soil temperatures for shallow geothermal applications in Turkey. Renewable and Sustainable Energy Reviews. 70, 71-77.

[9] Yadav, B. and Eliza, K. (2017) A hybrid wavelet-support vector machine model for prediction of Lake water level fluctuations using hydrometeorological data. Measurement. 103, 294-301.

[10] Sirsat, M.S., Cernadas, E., Fernandez-Delgado, M. and Khan, R. (2017) Classification of agricultural soil parameters in India. Computers and Electronics in Agriculture. 135, 269-279.

[11] Silvestro, P.C., Pignatti, S., Pascucci, S., Yang, H., Li, Z.H., Yang, G.J., Huang, W.J. and Casa, R. (2017) Estimating Wheat Yield in China at the Field and District Scale from the Assimilation of Satellite Data into the Aquacrop and Simple Algorithm for Yield (SAFY) Models. Remote Sensing, 9, 509-533.

[12] Shao, J., Meng, W. and Sun, G.D. (2017) Evaluation of missing value imputation methods for wireless soil datasets. Personal and Ubiquitous Computing. 21, 113-123.

[13] Shahabi, M., Jafarzadeh, A.A., Neyshabouri, M.R., Ghorbani, M.A. and Kamran, K.V. (2017) Spatial modeling of soil salinity using multiple linear regression, ordinary kriging and artificial neural network methods. Archives of Agronomy and Soil Science. 63, 151-160.
[14] Sabanci, K. and Aydin, C. (2017) Smart Robotic Weed Control System for Sugar Beet. Journal of Agricultural Science and Technology. 19, 73-83.
[15] Salem, G.S.A., Kazama, S., Komori, D., Shahid, S. and Dey, N.C. (2017) Optimum Abstraction of Groundwater for Sustaining Groundwater Level and Reducing Irrigation Cost. Water Resources Management. 31, 1947-1959.
[16] Huang, J., McBratney, A.B., Minasny, B. and Triantafilis, J. (2017) Monitoring and modelling soil water dynamics using electromagnetic conductivity imaging and the ensemble Kalman filter. Geoderma. 285, 76-93.
[17] Rahnemoonfar, M. and Sheppard, C. (2017) Deep Count: Fruit Counting Based on Deep Simulated Learning. Sensors. 17.
[18] Pineda, M., Perez-Bueno, M.L., Paredes, V. and Baron, M. (2017) Use of multicolour fluorescence imaging for diagnosis of bacterial and fungal infection on zucchini by implementing machine learning. Functional Plant Biology. 44, 563-572.
[19] Ostad-Ali-Askari, K., Shayannejad, M. and Ghorbanizadeh-Kharazi, H. (2017) Artificial neural network for modeling nitrate pollution of groundwater in marginal area of Zayandeh-rood River, Isfahan, Iran. KSCE Journal of Civil Engineering. 21, 134-140.
[20] Opena, H.J.G. and Yusiong, J.P.T. (2017) Automated Tomato Maturity Grading Using Abc-Trained Artificial Neural Networks. Malaysian Journal of Computer Science. 30, 12-26.
[21] Milacic, L., Jovic, S., Vujovic, T. and Miljkovic, J. (2017) Application of artificial neural network with extreme learning machine for economic growth estimation. Physica a-Statistical Mechanics and Its Applications. 465, 285-288.
[22] Lu, H., Fu, X., Liu, C., Li, L.G., He, Y.X. and Li, N.W. (2017) Cultivated land information extraction in UAV imagery based on deep convolutional neural network and transfer learning. Journal of Mountain Science. 14, 731-741.
[23] Leauthaud, C., Cappelaere, B., Demarty, J., Guichard, F., Velluet, C., Kergoat, L., Vischel, T., Grippa, M., Mouhaimouni, M., Bouzou Moussa, I., Mainassara, I. and Sultan, B. (2017) A 60-year reconstructed high-resolution local meteorological data set in Central Sahel (1950-2009): evaluation, analysis and application to land surface modelling. International Journal of Climatology. 37, 2699-2718.
[24] Xue, Z.H., Du, P.J., Li, J. and Su, H.J. (2017) Sparse graph regularization for robust crop mapping using hyperspectral remotely sensed imagery with very few in situ data. Isprs Journal of Photogrammetry and Remote Sensing. 124, 1-15.
[25] Kussul, N., Lavreniuk, M., Skakun, S. and Shelestov, A. (2017) Deep Learning Classification of Land Cover and Crop Types Using Remote Sensing Data. IEEE Geoscience and Remote Sensing Letters. 14, 778-782.
[26] Hussain, S. and Al Alili, A. (2017) A pruning approach to optimize synaptic connections and select relevant input parameters for neural network modelling of solar radiation. Applied Soft Computing. 52, 898-908.
[27] Guclu, Y.S., Subyani, A.M. and Sen, Z. (2017) Regional fuzzy chain model for evapotranspiration estimation. Journal of Hydrology. 544, 233-241.
[28] Giannikopoulou, A.S., Gad, F.K., Kampragou, E. and Assimacopoulos, D. (2017) Risk-Based Assessment of Drought Mitigation Options: The Case of Syros Island, Greece. Water Resources Management. 31, 655-669.
[29] Castaneda-Miranda, A. and Castano, V.M. (2017) Smart frost control in greenhouses by neural networks models. Computers and Electronics in Agriculture. 137, 102-114.
[30] Van Linden, V. and Herman, L. (2014) A fuel consumption model for off-road use of mobile machinery in agriculture. Energy. 77, 880-889.
[31] Khoshnevisan, B., Rafiee, S., Omid, M., Mousazadeh, H. and Rajaeifar, M.A. (2014) Application of artificial neural networks for prediction of output energy and GHG emissions in potato production in Iran. Agricultural systems. 123, 120-127.
[32] Zizala, D., Zadorova, T. and Kapicka, J. (2017) Assessment of Soil Degradation by Erosion Based on Analysis of Soil Properties Using Aerial Hyperspectral Images and Ancillary Data, Czech Republic. Remote Sensing. 9, 28-52.
[33] Yusof, M.F., Azamathulla, H.M. and Abdullah, R. (2014) Prediction of soil erodibility factor for Peninsular Malaysia soil series using ANN. Neural Computing and Applications. 24, 383-389.
[34] Saglam, C., Guzel, M. and Cetin, N. (2018) A Greenhouse Construction with Fiber-Reinforced Plastic Chords and Triangular Pyramid Models. Fresen. Environ. Bull. 27, 9447-9452.
[35] Baytorun, N., Akyüz, A. and Üstün, S. (2016) Expert System in Greenhouse Heating Systems "ISIGER-SERA". Journal of Mechanical Engineering. 155, 13-24. (in Turkish).

[36] Canakci, M., Emekli, N.Y., Bilgin, S. and Caglayan, N. (2013) Heating requirement and its costs in greenhouse structures: A case study for Mediterranean region of Turkey. Renewable and Sustainable Energy Reviews. 24, 483-490.
[37] Damrath, J. and Klein, L.F. (1983) Tables for heating energy of greenhouses Horticultural information 18. Institute of Technology in Horticulture and Agriculture. Hannover, 18. (in German).
[38] Damrath, J. (1980) Tables for determining the heating energy of greenhouses Horticultural information 8. Institute of Technology in Horticulture and Agriculture. Hannover, 8. (in German).
[39] Tantau, H.J. (1983) Heating systems in horticulture. Manual of the purchase gardener. Verlag Eugen Ulmer, Stuttgart, 1-258. (in German).
[40] Von Zabeltitz, C. (2011) Integrated Greenhouse Systems for Mild Climates: Climate Conditions, Design, Construction, Maintenance, Climate Control. Berlin, Springer, 285-311.
[41] Hallaire, M. (1950) Average night, day and daytime temperatures expressed as a function of daily minimum and maximum temperatures. Weekly Reports of Sessions of the Academy of Sciences. 231, 1533-1535. (in French).
[42] Rath, T. (1992) Use of knowledge-based systems for modelling and presentation of horticultural expertise using the example of the hybrid expert system HORTEX. Horticultural information (Germany). no. 34. (in German).
[43] Tantau, H.J. (2008) Heat consumption measurement - influencing factors. In: Report on the Determination and Assessment of the Energy Consumption of Greenhouses. KTBL Workshop. 17 September 2008. 22-30. (in German).
[44] Von Zabeltitz, C. (1986) Greenhouses - Guide of the purchase gardener. Ulmer-Verlag, Stuttgart. (in German).
[45] Öztemel, E. (2012) Artificial Neural Networks. Papatya Yayincilik, Istanbul, Turkey, 1-232. (in Turkish).
[46] Meyer, J. (2008) Nomenclature and definition. In: Report on the determination and evaluation of the energy needs of greenhouses. Board of Trustees for Engineering and Construction in Agriculture e. V., Darmstadt, 14-22. (in German).
[47] Demuth, H.B. and Beale, M.H. (2004) Neural network toolbox for use with MATLAB: User guide. Math Works, Natick, MA, USA, 1-846.
[48] Vogl, T.P., Mangis, J., Rigler, A., Zink, W. and Alkon, D. (1988) Accelerating the convergence of the back-propagation method. Biological cybernetics. 59, 257-263.
[49] Zhou, G. and Si, J. (1998) Advanced neural-network training algorithm with reduced complexity based on Jacobian deficiency. IEEE Trans Neural Netw. 9, 448-453.
[50] Tantau, H. (2012) Low Energy Greenhouse–Method to Analyse Heat Flux and PAR-Transmittance. Landtechnik, Building and Planning. 67, 196-204.

Received: **08.10.2018**
Accepted: **09.06.2019**

CORRESPONDING AUTHOR

Ali Cayli
Kahramanmaras Sutcu Imam University,
Vocational School of Turkoglu,
Kahramanmaras – Turkey

e-mail: alicayli@ksu.edu.tr